Free-radical crosslinking of specific proteins alters the function of the egg extracellular matrix at fertilization

Julian L. Wong and Gary M. Wessel*

All animal embryos begin development by modifying the egg extracellular matrix. This protein-rich matrix protects against polyspermy, microbes and mechanical stress via enzyme-dependent transformations that alter the organization of its constituents. Using the sea urchin fertilization envelope, a well-defined extracellular structure formed within minutes of fertilization, we examine the mechanisms whereby limited permeability is established within this matrix. We find that the fertilization envelope acquires a barrier filtration of 40,000 daltons within minutes of insemination via a peroxidase-dependent mechanism, with dynamics that parallel requisite production of hydrogen peroxide by the zygote. To identify the molecular targets of this free-radical modification, we developed an in vivo technique to label and isolate the modified matrix components for mass spectrometry. This method revealed that four of the six major extracellular matrix components are selectively crosslinked, discriminating even sibling proteins from the same gene. Thus, specific free-radical chemistry is essential for establishing the embryonic microenvironment of early development.

KEY WORDS: Dityrosine, Peroxidase, Permeability, Fertilization envelope, Hydrogen peroxide

INTRODUCTION

Upon fertilization, the animal zygote transforms the egg extracellular matrix into a protective physical structure that encloses the embryo in a microenvironment in which embryogenesis can occur (reviewed by Shapiro et al., 1989; Wong and Wessel, 2006a). In general, modifications of this matrix stabilize the protein barrier so that digestion by a 'hatching enzyme' is necessary before the embryo may escape to begin feeding (Barrett et al., 1971; D'Aniello et al., 1997; Fan and Katagiri, 2001; Katagiri et al., 1997; Kitamura and Katagiri, 1998; Lee et al., 1994; Lepage and Gache, 1990; Mozingo et al., 1993; Nomura et al., 1997; Sawada et al., 1990; Yamagami et al., 1992). The timing of hatching varies among animals, occurring at blastula for feeding embryos such as echinoderms, ascidians and mammals, or at birth for embryos whose store of yolk sustains them throughout development, such as teleosts, birds and reptiles.

The microenvironment enclosed upon creation of this zygotic extracellular matrix is established by at least two egg contributions. First, hydration of proteoglycans from egg vesicles establishes an aqueous cushion within the perivitelline space, the volume that distances the embryo from the barrier (Kay and Shapiro, 1985; Larabell and Chandler, 1991; Schuel et al., 1974; Shapiro et al., 1989; Talbot and Dandekar, 2003; Talbot and Goudeau, 1988). Second, the matrix itself is transformed by enzymes derived from the cortical granules, a process that alters the matrix characteristics to resist mechanical distortion and chemical dissolution (reviewed by Shapiro et al., 1989; Wong and Wessel, 2006a). In anurans, a zinc metalloprotease is responsible for the physicochemical alteration of their vitelline envelope (Lindsay and Hedrick, 2004); a functional homolog modifies the same target in the mammalian zona pellucida (Bauskin et al., 1999; Moller and Wassarman, 1989). Conversely, inter-protein crosslinks are essential for the change in extracellular matrix properties in insects (Li et al., 1996), teleosts (Chang et al., 2002; Kudo, 1988; Oppen-Berntsen et al., 1990) and echinoderms (Foerder and Shapiro, 1977; Hall, 1978; Wong et al., 2004). One or many of these biochemical modifications are hypothesized to establish a physical barrier separating the outside from the perivitelline space, thereby maintaining a sterile, or even a dessicant-resistant, microenvironment (Grey et al., 1974; Kay and Shapiro, 1985; Shapiro et al., 1989).

Two types of protein crosslinks are generally involved in the transformation of the egg extracellular matrix (Wong and Wessel, 2006a). Transglutaminase establishes covalent epsilon (gamma-glutamyl)lysine bonds in a calcium-dependent fashion in teleosts (Chang et al., 2002; Kudo, 1988; Oppen-Berntsen et al., 1990) and sea urchins (Battaglia and Shapiro, 1988). Peroxidase, however, forms dityrosine crosslinks via a free-radical mechanism (Davies, 1987; Davies and Delsignore, 1987; Davies et al., 1987; Gross, 1959; Heinecke et al., 1993a; Heinecke et al., 1993b; Yip, 1966) in insects (Li et al., 1996) and sea urchins (Foerder and Shapiro, 1977; Hall, 1978). The possible targets of both enzymes in the sea urchin fertilization envelope are well defined, and include rendezvin, an alternatively spliced gene whose vitelline layer (RDZ^{120}) and cortical granule isoforms (RDZ^{40}, RDZ^{60}, RDZ^{70}, RDZ^{90}) are rich in CUB domains, as well as SFE1, SFE9, and proteoliaisin, which are each enriched with tandem low-density lipoprotein receptor type A repeats (LDLrA) (Wong and Wessel, 2004; Wong and Wessel, 2006a). These proteins and their various domains represent a diverse population with which to test the target specificity of the crosslinking mechanisms. Here, we identify a mechanism whereby specific protein crosslinking within the sea urchin fertilization envelope establishes the limited permeability of this filtration barrier (Kay and Shapiro, 1985).

MATERIALS AND METHODS

Animals

Adult *Strongylocentrotus purpuratus* were obtained from Charles Hollahan (Santa Barbara, CA) and kept in 15°C artificial seawater (ASW) until needed. Adult *Lytechinus variegatus* were collected from Beaufort, NC (USA) and kept in 22°C ASW until needed. ASW was generated from

Department of Molecular Biology, Cellular Biology, and Biochemistry, Box G-L173, Brown University, Providence, RI 02912, USA.

*Author for correspondence (e-mail: rhet@brown.edu)

Instant Ocean (Aquarium Systems, Mentor, OH). Eggs and sperm were collected for use by intracoelomic injection of 0.5 M KCl. Eggs were passed twice over 100-μm nylon mesh before using. Sperm were collected dry, pelleted at 1000 *g* for 30 seconds, and stored on ice until needed.

Permeability assays
Fertilization envelope permeability was tested by measuring the diffusion of fluorophore-conjugated dextrans into the perivitelline space. As appropriate, eggs were dejellied in ASW acidified with HCl (pH 5.2) (*S. purpuratus*) or calcium-free seawater (CFSW; *L. variegatus*) for 10 minutes, then washed three times in normal ASW (pH 8.0) to equilibrate the pH. Fertilization without extracellular calcium was conducted in CFSW after washing eggs three times in the respective medium to equilibrate the cells. Sperm diluted into ASW containing egg jelly were used to inseminate eggs in ASW, CFSW, or 1 mM 3-aminotriazole (3-AT; Sigma-Aldrich, St Louis, MO) in ASW; eggs were then incubated for 20 minutes. Zygotes were transferred to Kiehart chambers (Kiehart, 1982) containing 5 μM of both anionic Cascade Blue dextran (3000 daltons) and one neutral Texas Red dextran of 3000, 10,000, 40,000 or 70,000 daltons (Invitrogen, Carlsbad, CA) diluted in ASW. Ten minutes after exposure to the chamber, zygotes were imaged at the equatorial plane of each fertilization envelope for both the Cascade Blue and Texas Red fluorophores, on a TCS SP2 AOBS confocal scanning microscope driven by proprietary software (Leica Microsystems, Bannockburn, IL). Average fluorescence intensity was measured over three random regions (30 pixel diameter) within the perivitelline space or the surrounding medium using Metamorph software (Universal Imaging Corporation, Downingtown, PA). Average Texas Red measurements per zygote were normalized to Cascade Blue measurements per region per sample, and the percentage of labeling in the perivitelline space versus the media was calculated per region. Average percentages over three regions per zygote were used to compare the population across 7-10 zygotes per treatment. Two-tailed Student's *t*-tests were used to evaluate significance per treatment compared with normal fertilization.

Localization and quantification of dityrosine formation
Peroxidase-mediated catalysis of dityrosine crosslinks within the fertilization envelope was tracked with the fluorescent conjugates tyramide-Alexa Fluor 488 and -Alexa Fluor 594 (Molecular Probes, Eugene, OR). Stock solutions of tyramide-Alexa Fluor (made according to manufacturer's instructions; the final concentrations are proprietary, thus we refer to the concentrations as dilutions of this stock) were used in all experiments. A final concentration of 1 mM 3-AT was used to inhibit ovoperoxidase as necessary. Static imaging of the Alexa Fluor conjugates was accomplished on a Zeiss LSM410 confocal laser-scanning microscope (Carl Zeiss Corporation, Thornwood, NY) using RENAISSANCE software (Microcosm, Columbia, MD).

Quantification of tyramide-Alexa Fluor 488 incorporation within the fertilization envelope was achieved by fertilizing eggs in the presence of a 1:200 dilution of the fluorochrome conjugate, as previously published (Wong et al., 2004). Thirty minutes after insemination, the cells were washed twice with ice-cold ASW, and then stored on ice until visualization. Confocal microscope images containing optical cross-sections of fertilization envelopes at the equator were analyzed with Metamorph software (Universal Imaging Corporation, Downingtown, PA). Fluorescence intensity was quantified as a ring from the cell surface to the outside of the fertilization envelope: Total fluorescence intensity (I) and total area (A) were measured in circular regions five pixels either outside the fertilization envelope (FE) or along the cell plasma membrane (CELL). Measurements for each species were normalized according to the following formula:

$$\text{Fluorescence intensity} = (I_{FE} - I_{CELL}) / (A_{FE} - A_{CELL}).$$

Averages of at least 12 individual zygotes per species are reported for each treatment.

Time-lapse confocal microscopy was used to identify *S. purpuratus* ovoperoxidase activity in vivo during fertilization envelope formation. For these experiments, eggs were loaded into Kiehart chambers (Kiehart, 1982) with a final concentration of 1 μM FM1-43 (Molecular Probes), to label the cell membrane, and a tyramide-Alexa Fluor 594 at a final dilution of

1:16,000. Eggs within the chamber were inseminated with 4 μl of a 1:100 dilution of sperm (1:10,000 final dilution). The field was then scanned every 10 seconds for the membrane marker FM1-43 and tyramide-Alexa Fluor 594 accumulation using a TCS SP2 AOBS confocal scanning microscope (Leica Microsystems, Bannockburn, IL). The time when fertilization occurred (*t*=0) was determined by DIC images, and a corresponding rise in FM1-43 fluorescence intensity at the cell surface (Voronina and Wessel, 2004). Tyramide-Alexa Fluor 594 incorporation was then measured as fluorescence intensity within the fertilization envelope per frame, as above. Net fluorescence was calculated by subtracting background fluorescence values at the image just prior to fertilization (*t*=−10 seconds). Time series data sets per egg were normalized to the maximum fluorescence after 10 minutes (600 seconds) of recording.

Labeling of ovoperoxidase substrates within the fertilization envelope
S. purpuratus eggs were equilibrated to 5 mM tyramine HCl and various stock dilutions of either tyramide-Alexa Fluor 594 or tyramide-DSB biotin (Invitrogen) dissolved in ASW before insemination. Thirty minutes after insemination, zygotes were gently washed twice with ASW. Fertilization envelopes were recovered from zygotes by passing them through a 64-μm nylon mesh to separate the tyramine-softened fertilization envelopes (tyramine-SFEs) from the cells. Cells were settled by gravity on ice, and the soft fertilization envelopes (SFEs) in the supernatant were collected by centrifugation at 10,000 *g*. SFEs were washed once with water and then resuspended in 10 mM Tris, 50 mM EDTA, pH 8.0. This resuspension was stored at −80°C until needed.

In vitro crosslinking of soft fertilization envelopes
S. purpuratus eggs were preincubated in 10 μM diphenyleneiodonium (DPI; Sigma-Aldrich) and then fertilized as described previously (Wong et al., 2004). Non-crosslinked FEs from this method of inhibition (DPI-SFEs) were separated and purified from zygotes with nylon mesh, as above, and stored in a concentrated form in ASW at 4°C on ice until needed. Samples treated with inhibitors such as 3-AT or DPI were incubated for 10 minutes at room temperature prior to the addition of hydrogen peroxide. Various competitors, such as tyramine or tyramide analogs, were included in specific experiments, as noted in figures. Crosslinking was achieved by addition of exogenous hydrogen peroxide (10 nM to 10 μM final concentration) diluted in ASW at room temperature. Following 20 minutes of hydrogen peroxide exposure, each sample was washed twice in a 10-fold excess of ASW. Treated SFEs were pelleted at 10,000 *g* for 5 minutes, and stored dry at −80°C until needed.

Identification of ovoperoxidase protein targets within the fertilization envelope
Sixty micrograms of each SFEs sample was subjected to SDS-PAGE on pre-cast 4-20% polyacrylamide Tris-Glycine gels (Life-Therapeutics, Frenchs Forest, New South Wales, Australia). Alexa Fluor 594 fluorescence was recorded using a Typhoon fluorescent scanner run by proprietary software (Amersham Biosciences, Piscataway, NJ). The gel was subsequently stained with Coomassie Blue to check loading.

Alternatively, the separated proteins were transferred to nitrocellulose for detection of DSB-biotin labeling (60 μg each SFE sample) or individual components of the sea urchin extracellular matrix (2 μg each SFE sample). Blots destined for DSB-biotin detection were blocked in 1% BSA in TBST [170 mM NaCl, 50 mM Tris, 0.05% Tween20 (v/v), pH 8.0], then probed overnight with Extravidin-AP (1:300,000 dilution; Sigma-Aldrich). Immunoblots were blocked in Blotto [3% non-fat dry milk (w/v), 170 mM NaCl, 50 mM Tris, 0.05% Tween20 (v/v)], and then probed overnight with rabbit antisera against proteoliaisin (Somers et al., 1989; Somers and Shapiro, 1991), SFE1 (Wessel et al., 2000a), SFE9 (Wessel, 1995), separate epitopes of rendezvin (Wong and Wessel, 2006b), ovoperoxidase (LaFleur, Jr et al., 1998), or fertilization envelope-incorporated vitelline layer (J.L.W. and G.M.W., unpublished). These immunoblots were washed twice with Blotto, then incubated with alkaline phosphatase-conjugated goat anti-rabbit IgG (Sigma-Aldrich), diluted 1:30,000 in Blotto, for 1 hour. All blots were washed extensively in TBST, and then in alkaline phosphatase buffer (100 mM NaCl, 5 mM MgCl₂, 100 mM Tris, pH 9.5). Immunoreactivity of the

secondary antibody was detected by 5-bromo-4-chloro-3-indolyl phosphate/nitro blue tetrazolium (BCIP/NBT), as previously described (McGadey, 1970).

Tandem mass spectrometry analysis

Fluorescently tagged bands were excised from SDS-PAGE gels, and sent to the COBRE Center for Cancer Research Development at Lifespan/Brown University for processing. Following tryptic digestion, proteins in gel samples (Josic et al., 2005) were eluted directly into a QSTAR XL hybrid qTOF mass spectrometer (Applied Biosystems, Foster City, CA and Sciex, Concord, Ontario, Canada) via electrospray ionization (Josic et al., 2006; Wilm et al., 1996). LC-MS spectra were analyzed using MASCOT software (Perkins et al., 1999).

RESULTS
Fertilization envelope permeability

Fluorophore-conjugated dextrans were used to test the permeability of the fertilization envelope. Unlike proteins, neutral dextrans do not adhere to the surface of the matrix and larger dextran polymers achieve a range of secondary structures whose Stoke's radius increases proportionally with molecular mass (Persky and Hendrix, 1990). Furthermore, although barriers examined in mammals show increased permeability to some serum proteins compared with exogenous proteins or dextrans of similar molecular mass (Ambati et al., 2000; Parr and Parr, 1986), the osmolarity of the sea urchin media caused similar globular proteins to adhere to the fertilization envelope (data not shown), possibly altering its filtration dynamics.

We therefore used various dextrans. The diffusion of Texas Red-labeled dextrans of various molecular mass across the fertilization envelope and into the perivitelline space was compared with the passage of 3000 dalton Cascade-Blue dextran. Both *Strongylocentrotus purpuratus* and *Lytechinus variegatus* fertilization envelopes possess a diffusion cut-off of 50% with 30,000- to 50,000-dalton dextrans (Fig. 1), a shared threshold that is consistent with their orthologous constituents (Wong and Wessel, 2004). This molecular permeability of the acellular fertilization envelope matrix is similar to limits determined for the mammalian sclera (Ambati et al., 2000) and the cell-mediated endometrial decidual zone at the site of implantation (Parr and Parr, 1986).

We next tested how perturbations to the formation of the fertilization envelope affect filtration dynamics. A fertilization envelope assembled in calcium-free seawater is morphologically similar to the original, highly permeable vitelline layer (Carroll et al., 1986; Cheng et al., 1991). The source of this open architecture is likely to be the decreased cohesion of the structural proteins in the absence of calcium (Hall, 1978), and is thus a control for the loss of restricted permeability. In addition, the absence of calcium represses transglutaminase-dependent crosslinking (Ha and Iuchi, 1998; Lorand and Graham, 2003; Zanetti et al., 2004), allowing us to avoid the typical competitive substrate inhibitors for transglutaminase, such as cadaverine, putresceine and glycine ethyl esters (Battaglia and Shapiro, 1988), which all have potential steric effects that could affect filtration dynamics. By contrast, direct
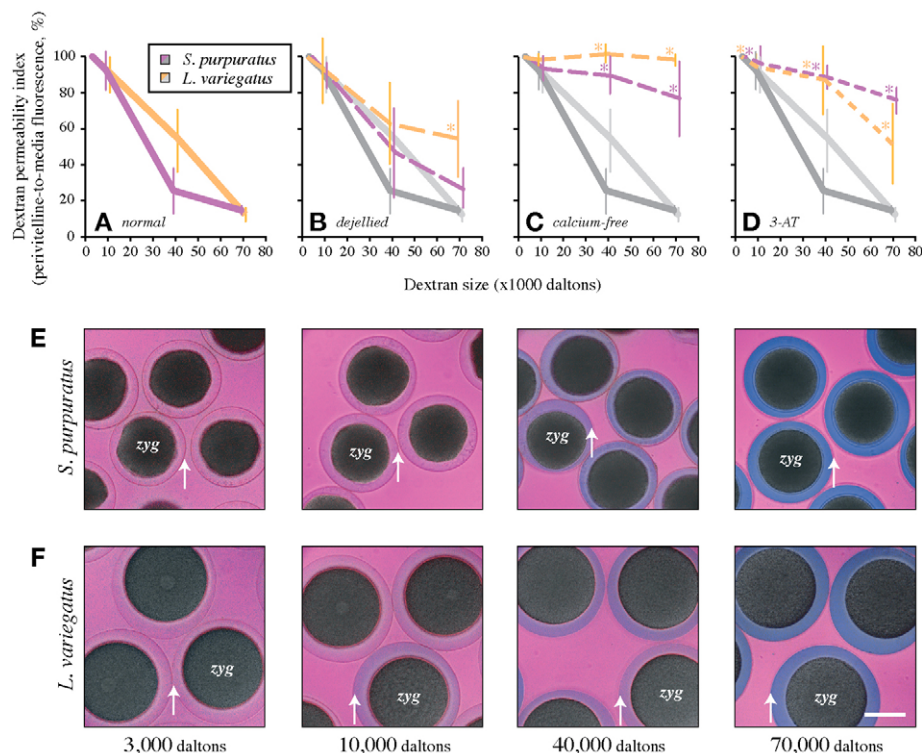
Fig. 1. Peroxidase-mediated crosslinking in the sea urchin fertilization envelope contributes to its permeability barrier. (**A-D**) Plots show permeability of dextrans into the perivitelline space of zygotes whose embryos were formed as normal (A), after egg dejellying (B), in calcium-free seawater (C), and in 3-AT (D). Plots show the percentage of normalized fluorescence (variable molecular mass Texas Red dextran fluorescence to control 3,000-dalton Cascade Blue dextran) within the perivitelline space versus the media outside the zygote. At least seven individuals were measured for each point plotted. Mean percentages and standard deviation are shown. Data from normal formation conditions (A) are reproduced in greyscale in other plots (B-D). Significant changes in permeability compared with normal zygotes ($P<10^{-10}$) are indicated (asterisks). (**E,F**) Merged images of fertilization envelopes formed under normal conditions for *S. purpuratus* (E) and *L. variegatus* (F). Neutral Texas Red dextran fluorescence (3,000 to 70,000 daltons; red) overlaid with control Cascade-Blue dextran (3,000 daltons; blue), on top of DIC images (greyscale). Perivitelline space is found between the zygote (zyg) and the fertilization envelope (arrow). Scale bar: 50 μm.

inhibitors of ovoperoxidase, such as 3-aminotriazole (3-AT) (Foerder and Shapiro, 1977), enabled us to test the effects of dityrosine crosslinks on permeability. In the absence of calcium (Fig. 1C) or ovoperoxidase activity (Fig. 1D), the corresponding fertilization envelopes are no longer restrictive to the higher molecular mass dextrans. Furthermore, the specificity of 3-AT for ovoperoxidase activity (Foerder and Shapiro, 1977) suggests that dityrosine crosslinks restrict 30-60% diffusion of the high molecular mass dextans across the fertilization envelope. Despite the facilitated delivery of 70,000-120,000 dalton biomolecules upon inhibition of ovoperoxidase, the physical presence and charge of the fertilization envelope still limit the accessibility of larger biomolecules (e.g. DNA, RNA or proteins, such as immunoglobulins; J.L.W. and G.M.W., unpublished) to the embryo; only complete removal of the fertilization envelope will ensure maximal embryo exposure.
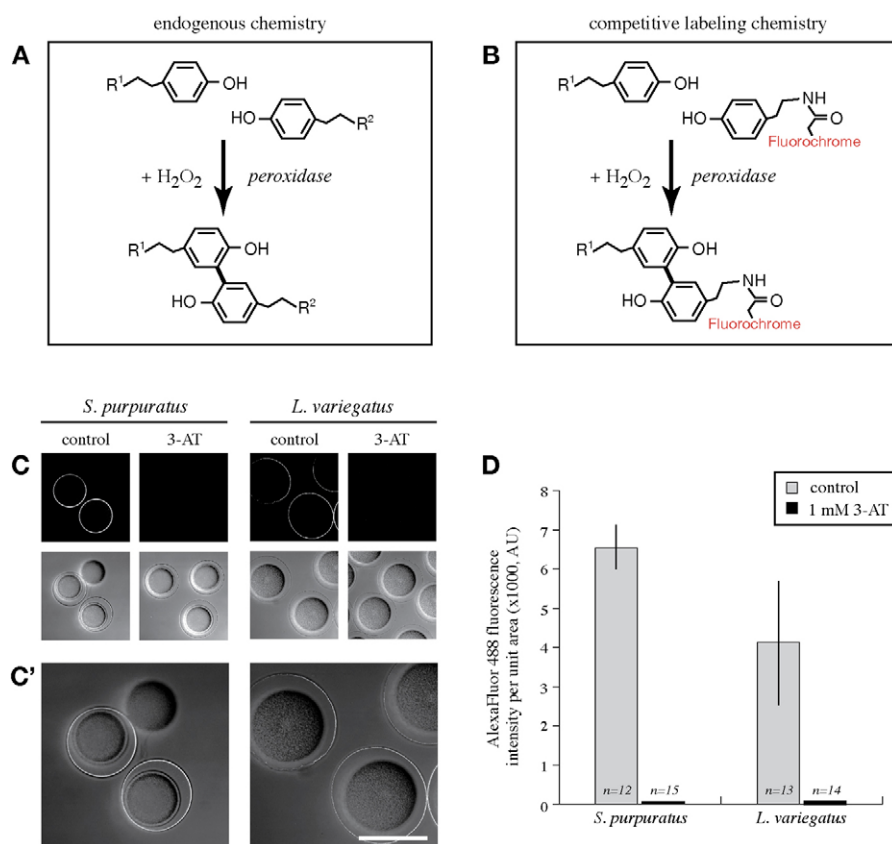
In vivo imaging of dityrosine crosslink formation

We next sought to identify the ovoperoxidase substrates that are targeted for crosslinking. First, we used tyramide-fluorochrome conjugates (Fig. 2B) (Bobrow et al., 1989; Bobrow et al., 1991; Hunyady et al., 1996) to visualize the in vivo targets of the endogenous sea urchin ovoperoxidase. Inclusion of tyramide-Alexa Fluor in media during fertilization of either *S. purpuratus* or *L. variegatus* eggs resulted in the selective accumulation of fluorochrome within the fertilization envelope, but not at the egg surface (Fig. 2C). Labeling with tyramide-Alexa Fluor is abolished in the presence 3-AT (Fig. 2C,D) (Showman and Foerder, 1979), consistent with the localization of ovoperoxidase to the fertilization envelope following cortical granule exocytosis (Mozingo et al., 1994; Somers et al., 1989).

Time-lapse imaging of fertilization in the presence of tyramide-fluorochrome conjugates revealed a biphasic activity curve for *S. purpuratus* ovoperoxidase (Fig. 3). Enzyme crosslinking is linear for about 275 seconds following fertilization, and then plateaus over the remaining 225 seconds; the time to 50% completion is approximately 140 seconds (Fig. 3B). This biphasic profile is a direct effect of hydrogen peroxide synthesis by Udx1 (Wong et al., 2004), such that the linear phase overlaps the most abundant production of hydrogen peroxide and the lagging phase corresponds to the depression of Udx1 activity (Fig. 3B). Thus, the rate-limiting step of ovoperoxidase crosslinking of fertilization envelope proteins is the availability of its primary substrate. Although the majority of the detectable nine million molecules of hydrogen peroxide synthesized by a single embryo (Wong et al., 2004) is used to establish dityrosine crosslinks, not all of these molecules are consumed by ovoperoxidase; the remainder may be used in cell signaling (Wong and Wessel, 2005), as a catalytic 'sterilizing' agent (Klebanoff et al., 1979), or may simply decay during its diffusion away from the embryo.

Identification of endogenous ovoperoxidase targets

Isolation and identification of peroxidase substrates requires that the targets be soluble, yet a common outcome of crosslinking is matrix insolubility – as exemplified by the gel mobility of the fertilization envelope constituent SFE9 (Wessel, 1995). To counter this, we used competitive substrates that formed free tyrosyl radicals (Gulyas and Schmell, 1980; Jacob et al., 1996) to inhibit endogenous, inter-protein dityrosine crosslinking. We first tested the effects of free L-tyrosine, but, as noted previously (Hall, 1978), its low solubility in media proved problematic. In the presence of

Fig. 2. In vivo incorporation of tyramide-conjugates identifies endogenous ovoperoxidase activity. (**A**) The chemistry of peroxidase-mediated formation of dityrosine crosslinks between adjacent proteins (R^1, R^2). This chemistry can be exploited to permanently bind a fluorochrome to proteins, as per the tyramide signal amplification mechanism (Bobrow et al., 1989). (**B**) The tyramide-fluorochrome conjugates compete with the formation of endogenous dityrosine crosslinks. (**C**) Eggs pretreated with the ovoperoxidase inhibitor 3-aminotriazole (3-AT; right) (Showman and Foerder, 1979) show significantly less tyramide-Alexa Fluor 488 incorporation in the fertilization envelope than untreated controls (left). Fluorescence images (top) are complemented by DIC images (bottom). (**C'**) Fluorescence images from C overlaid on respective DIC images to show selectivity of incorporation. Scale bar: 100 μm. (**D**) Quantification of fluorescence intensity between control and 3-AT treated eggs. Mean fluorescence per unit area (AU, arbitrary units) at the equator of the fertilization envelope of each species. Standard deviation per treatment is shown. The number of replicates measured per treatment is indicated.
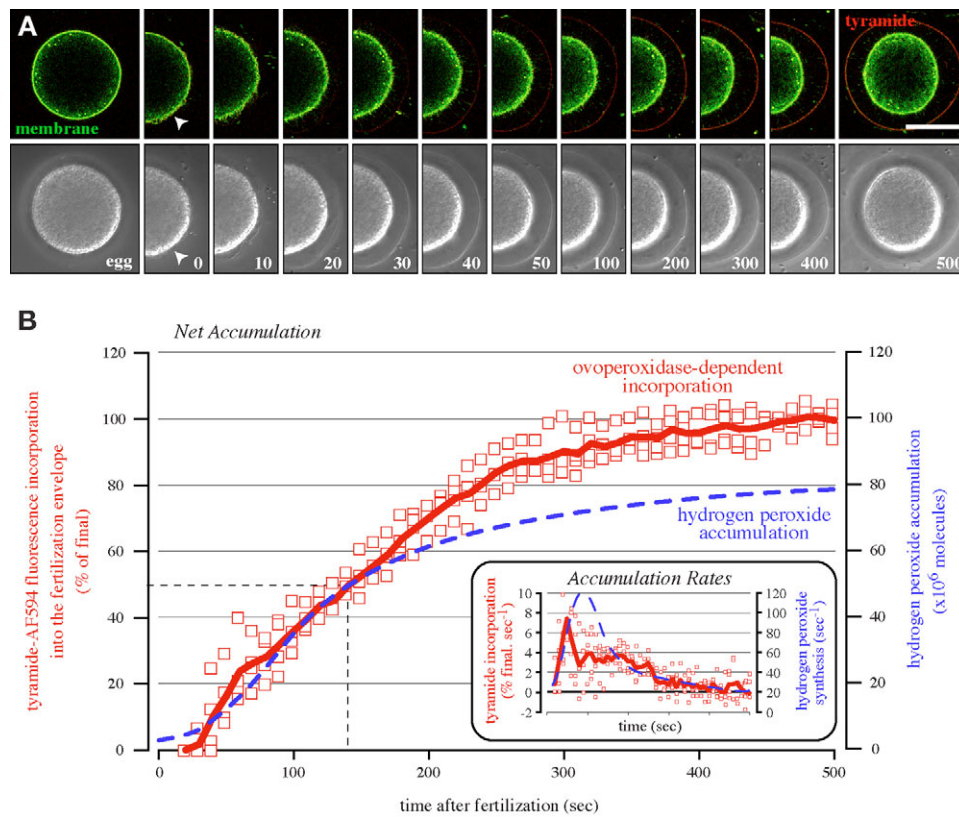
Fig. 3. Kinetics of ovoperoxidase crosslinking is linked to hydrogen peroxide synthesis. The incorporation of fluorescent tyramide analogs can be visualized in real time, and is limited to the fertilization envelope. (**A**) Representative snapshots of *Strongylocentrotus purpuratus* fertilization at times shown, where sperm fusion (arrowhead) represents time=0 (seconds). The concentration of tyramide-Alexa Fluor 594 (red) within the fertilization envelope (arrowhead) increases over time. The plasma membrane is counter-stained with FM1-43 (green). Fluorescence images (top) are complemented by DIC images (bottom). Scale bar: 50 μm. (**B**) Quantification of tyramide-Alexa Fluor 594 incorporation into the fertilization envelope (red) versus hydrogen peroxide production over time (blue) (Wong et al., 2004). Mean accumulation of tyramide fluorescence in the fertilization envelope shown (solid line); squares represent individual data sets per egg (total shown, *n*=4). Inset: Rate of tyramide-Alexa Fluor 594 incorporation into the fertilization envelope, as a proxy for ovoperoxidase activity (red), versus rate of hydrogen peroxide production by Udx1 (blue) (Wong et al., 2004). Plots show the percentage of final fluorescence intensity (tyramide-Alexa Fluor 594) or the maximal rate of hydrogen peroxide synthesis.

the tyramide-fluorochrome precursor tyramine, however, we observed a specific and dose-dependent increase in SFE9 gel mobility compared with the soluble loading control YP30 (Wessel et al., 2000b). The performance of 5 mM tyramine is equal to the inhibition of ovoperoxidase activity achieved with 1 mM 3-AT (Showman and Foerder, 1979) (see Fig. S1 in the supplementary material); indeed, we were able to separate these tyramine-treated soft fertilization envelopes (tyramine-SFEs) from the zygotes or embryos with gentle mechanical shearing (see Fig. S2A in the supplementary material). Furthermore, the presence of excess tyramine does not affect the retention of tyramide-Alexa Fluor in the fertilization envelope (see Fig. S2 in the supplementary material).

Electrophoresis of tyramine-SFEs identified a single protein heavily crosslinked by ovoperoxidase when these SFEs were formed in the presence of tyramide-Alexa Fluor (Fig. 4A, dashed box). Mass spectrometry of the fluorescently labeled protein resulted in 14 peptide matches within the predicted RDZ[120] open reading frame, not including the carboxyl terminal sequence enriched in 'PYQ' tyrosine-rich repeats (Fig. 4B). Probing tyramine-SFEs with antibodies against the amino- (represented by RDZ anti-αγδ) or carboxy-domains (RDZ anti-θ) of rendezvin (Wong and Wessel, 2006b) shows that only the carboxyl terminus of rendezvin (RDZ[120]

co-migrates with this fluorescent band. To determine if this is true in situ, we used an unbiased crosslinking assay probing whole cell homogenates of zygotes fertilized in the presence of either the direct ovoperoxidase inhibitor 3-AT or the dual oxidase inhibitor diphenyleneiodonium (DPI), which indirectly inhibits ovoperoxidase crosslinking by blocking substrate availability (Showman and Foerder, 1979; Wong et al., 2004). Under these conditions, the gel mobility of the vitelline layer-associated protein RDZ[120] is impaired when ovoperoxidase activity is present, thus supporting its role as a major substrate of this peroxidase (Wong and Wessel, 2006b). RDZ[60] and RDZ[90], however, are not substrates of ovoperoxidase, revealing distinct selectivity in the target recognition of this enzyme.

We also developed a semi-in vivo crosslinking assay to assess the mechanism of fertilization envelope modification. We used the observation that fertilization envelope constituents remain in complex following isolation in the absence of ovoperoxidase activity (Wong and Wessel, 2006b). Pliable fertilization envelopes were isolated in the presence of DPI so that ovoperoxidase was not affected, and then exposed to exogenous hydrogen peroxide for 20 minutes (Fig. 5A) to simulate the timing of Udx1 activity in vivo (Wong et al., 2004). This semi-in vivo system significantly enhanced the sensitivity with which the target population could be identified
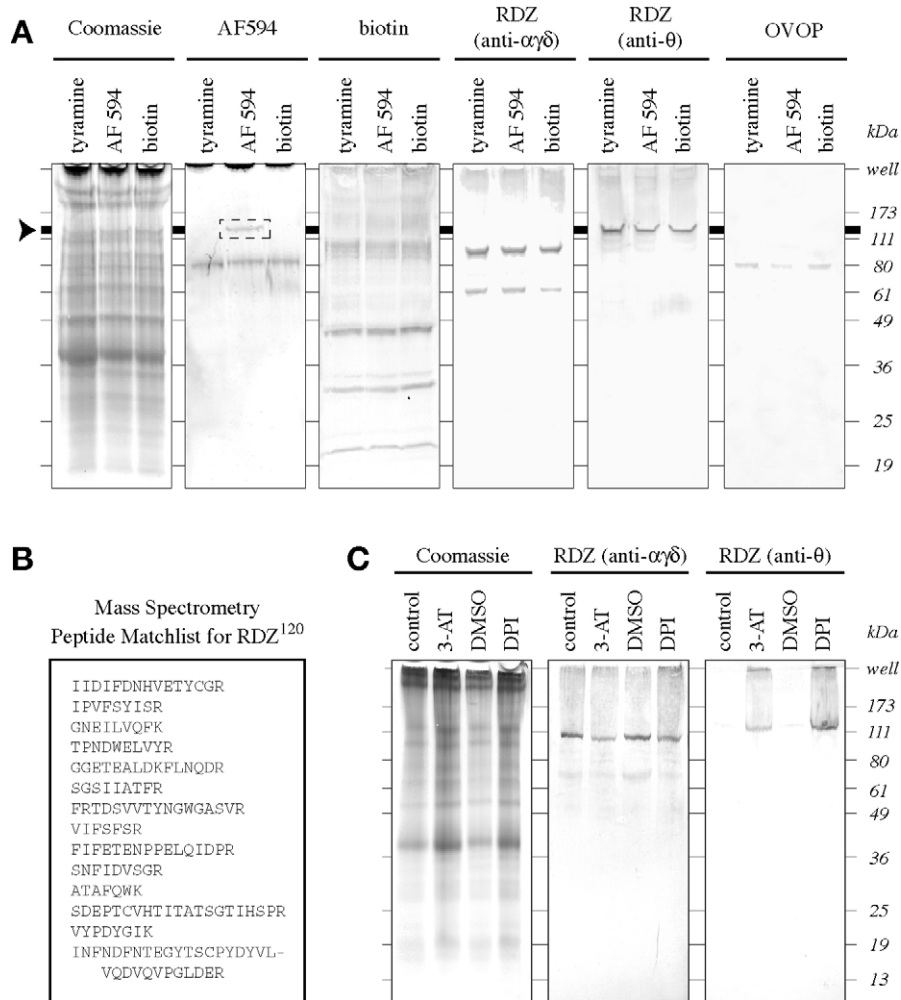
Fig. 4. Identification of ovoperoxidase target proteins labeled in vivo. (**A**) Fertilization envelopes isolated from embryos fertilized in the presence of 5 mM tyramine alone, or with tyramide-Alexa Fluor 594 or tyramide-biotin (1:100 dilution each) were separated by SDS-PAGE. Sixty micrograms of purified fertilization envelopes were used for Coomassie staining, the identification of Alexa Fluor 594 fluorescence, and detection of biotinylated bands. Antisera for rendezvin (RDZ) epitopes or for ovoperoxidase (OVOP) were used to probe 2 μg purified fertilization envelope proteins by immunoblot to identify the major target of ovoperoxidase-dependent dityrosine crosslinking (arrowhead). The major fluorescently labeled protein is boxed. (**B**) List of unmodified peptide matches to rendezvin[120] from mass spectrometry analysis of fluorescently labeled band from the fertilization envelopes (boxed band from A). (**C**) Fifty micrograms of total zygote lysates fertilized in the presence or absence of 3-AT or the Udx1 inhibitor diphenyleneiodonium (DPI), which abolishes synthesis of the ovoperoxidase substrate hydrogen peroxide (Wong et al., 2004), were separated by SDS-PAGE, and then stained with Coomassie or immunoblotted for different rendezvin (RDZ) epitopes. RDZ anti-αγδ is against the amino-terminal fragment whereas RDZ anti-θ is against the carboxy-terminal portion.

without compromising ovoperoxidase function, as revealed by the select labeling of the slower-migrating components proteoliaisin, SFE1 and SFE9 (Fig. 5B,C). The visualization of LDLrA-containing proteins (Wong and Wessel, 2004) as ovoperoxidase targets is consistent with previous observations (Wessel, 1995) and supports our mass spectrometry data obtained for a high molecular mass complex (data not shown). Again, neither RDZ[60] nor RDZ[90] are crosslinked under the physiological concentrations of hydrogen peroxide used (Fig. 5D), further reinforcing the molecular selectivity of ovoperoxidase activity.

DISCUSSION

Covalent crosslinking of extracellular matrix proteins is an essential mechanism used by cells throughout the animal kingdom. For example, maturation of the *Caenorhabditis elegans* cuticle (Edens et al., 2001) and production of active thyroid hormone by thyrocytes (Dunn and Dunn, 2001; Yip, 1966) both rely on peroxidase-mediated crosslinking events for normal function. Pathologically, pulmonary fibrosis resulting from excess dityrosine crosslinked lesions between collagen and elastin have been linked to transforming growth factor beta 1 (TGFβ1)-stimulated peroxidase release from lung fibroblasts during local inflammation (Larios et al., 2001), whereas atherosclerosis is associated with excess spurious tyrosyl conjugates generated by myeloperoxidase released from neutrophils at a site of inflammation (Heinecke, 1999; Heinecke et al., 1993a; Heinecke et al., 1993b; Jacob et al., 1996). The reactive

free radicals formed by this enzyme family are also correlated with molecular damage linked to aging (Bergendi et al., 1999; Fridovich, 1998; Levine and Stadtman, 2001; Linton et al., 2001).

Peroxidase-catalyzed protein crosslinks are formed by covalently joining the phenyl rings of adjacent tyrosine residues, making the resultant structure more resistant to chemical and mechanical forces (Harvey, 1909; Li et al., 1996). Although the formation of di- and tri-tyrosine conjugates have been identified by methods such as endogenous ultraviolet absorbance, chromatography and mass spectrometry (Heinecke, 1999; Heinecke et al., 1993a; Heinecke et al., 1993b; Jacob et al., 1996; Larios et al., 2001), the identity of the parent extracellular matrix targets remains a mystery. In fact, the free radical intermediate (Davies and Delsignore, 1987; Davies et al., 1987) suggests that the mechanism of crosslinking simply depends on the abundance and accessibility of tyrosine residues, rather than on peroxidase target specificity. Within the sea urchin fertilization envelope, however, the free radical chemistry is clearly selective. In contrast to the apparent promiscuity of ovoperoxidase to exogenous substrates such as bovine serum albumin (Klebanoff et al., 1979), we find here that only a subset of the endogenous fertilization envelope proteins are in vivo substrates. Indeed, sibling proteins, resulting from differentially spliced rendezvin mRNAs (Wong and Wessel, 2006b), are differentially crosslinked within the fertilization envelope. This preference for proteins – versus halides (Morrison and Schonbaum, 1976), free amino acids (Gross, 1959) or lipids (Levine and Stadtman, 2001) – is likely a consequence of tyrosyl
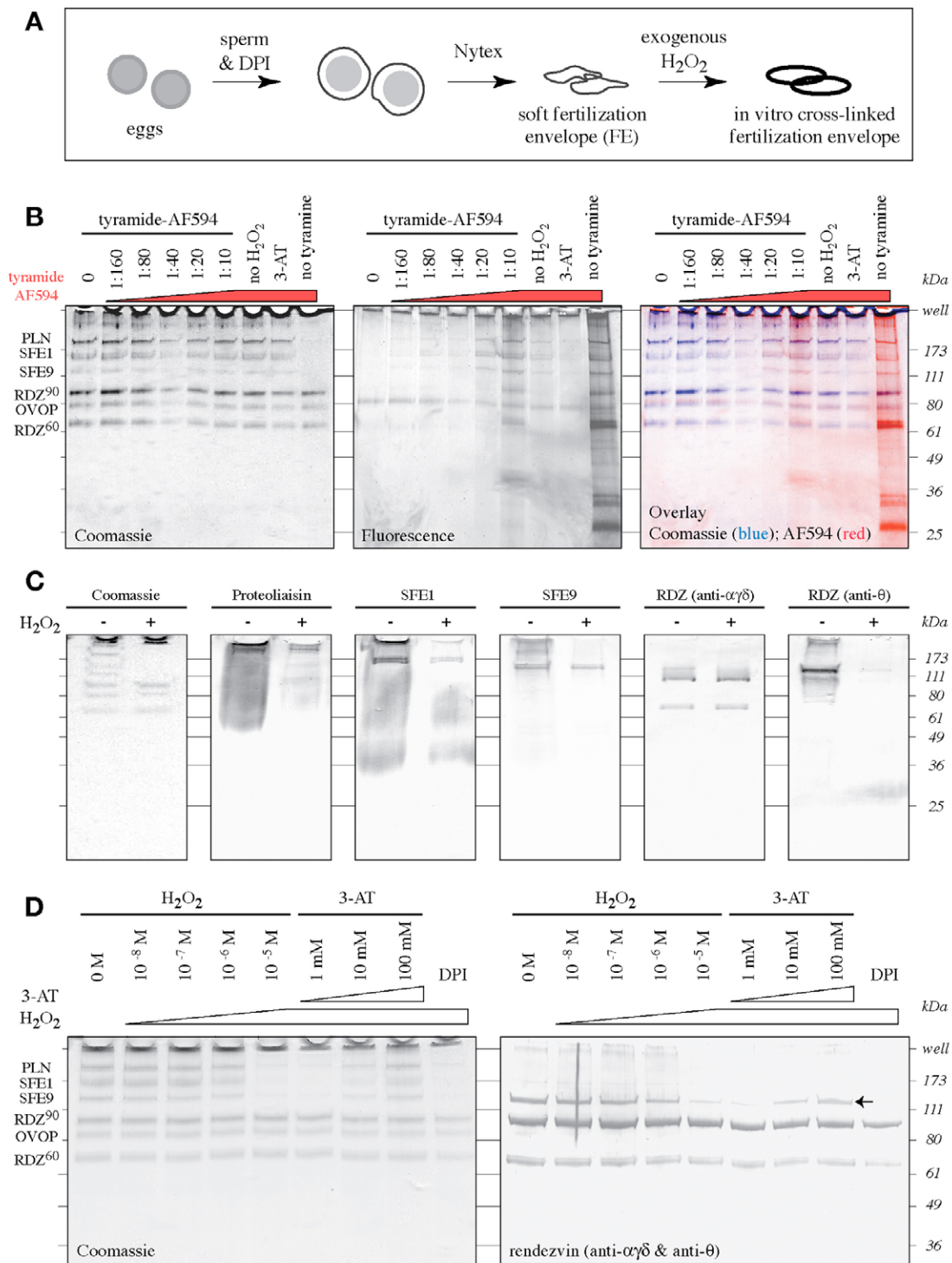
Fig. 5. Semi-in vivo crosslinking identifies four major targets of ovoperoxidase. (**A**) Isolation scheme for in vitro crosslinking assay, based on the ability to inhibit ovoperoxidase-dependent crosslinking using diphenyleneiodonium (DPI). (**B**) Titration of tyramide-Alexa Fluor 594 incorporation using the in vitro crosslinking assay from A. Fifty micrograms of DPI-isolated SFEs were reacted with various concentrations of tyramide-Alexa Fluor 594 in the presence of 10 mM tyramine (unless noted) and 10 μM hydrogen peroxide. Two-fifths (20 μg) of each reaction was separated by SDS-PAGE, and then visualized for Alexa Fluor 594 fluorescence (red) prior to staining with Coomassie (blue). Images were overlaid in pseudocolor to identify fluorescently labeled proteins (purple). Coomassie staining identifies the major fertilization envelope bands, including proteoliaisin (PLN), SFE1, SFE9, rendezvin isoforms (RDZ^{60}, RDZ^{90}) and ovoperoxidase (OVOP). (**C**) DPI-SFEs were in vitro crosslinked using 10 μM H$_2$O$_2$, and then separated by SDS-PAGE. Gels were stained for total protein (5 μg, Coomassie) or immunoblotted for individual fertilization envelope components (1 μg). (**D**) Titration of in vitro fertilization envelope crosslinking of rendezvin. Five micrograms of DPI-SFEs were exposed to serial dilutions of hydrogen peroxide (maximum of 10 μM H$_2$O$_2$) in the presence or absence of the inhibitors 3-AT (1-100 mM) or DPI (10 μM). One-fifth (1 μg) of each reaction was separated by SDS-PAGE and either stained with Coomassie or immunoblotted for rendezvin (RDZ). Individual Coomassie bands of structural fertilization envelope proteins are labeled. Arrow indicates rendezvin[120].
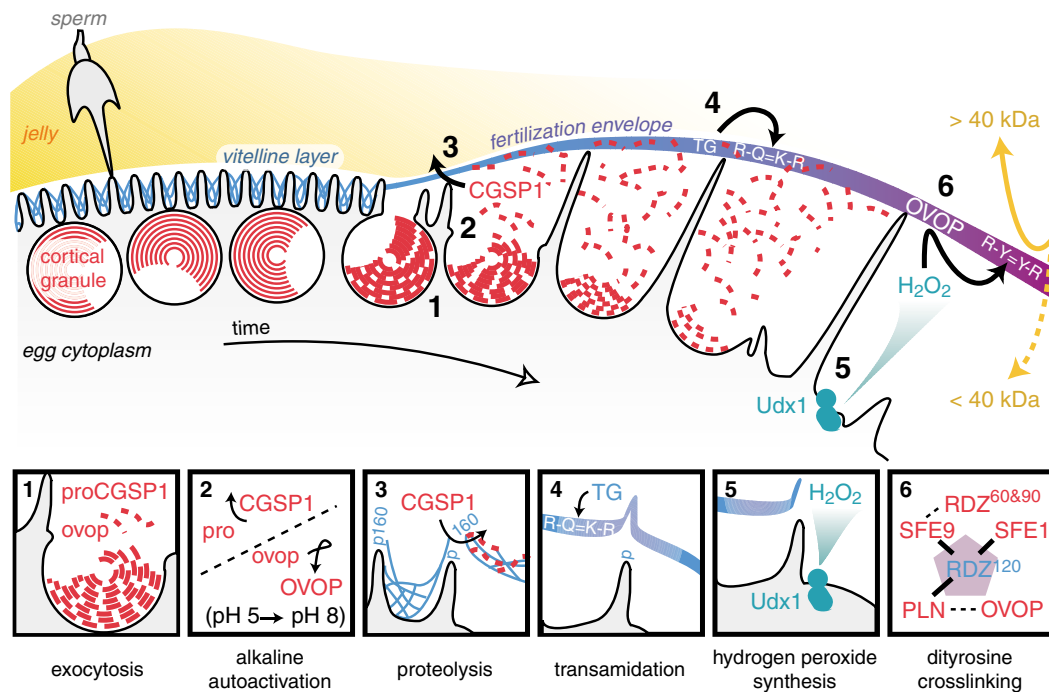
Fig. 6. Chronology of fertilization envelope formation. Diagram of the time-course of fertilization envelope assembly and modification of the egg cortex, starting from sperm fusion to ovoperoxidase-dependent crosslinking. Milestones (1-6) are detailed in the text. In panel 6, the dashed line denotes non-covalent interaction whereas the solid line denotes dityrosine crosslinking between proteins. CGSP1, cortical granule serine protease 1 (proCGSP1 indicates the zymogenic form); OVOP, ovoperoxidase (ovop indicates the zymogenic form); TG, transglutaminase; Udx1, urchin dual oxidase 1; RDZ, rendezvin; PLN, proteoliaisin; H_2O_2, hydrogen peroxide; "R-Q=K-R", covalent epsilon (gamma-glutamyl)lysine bonds; "R-Y=Y-R", covalent dityrosine crosslink; 40 kDa, macromolecules of 40,000 daltons.

abundance and availability within the fertilization envelope, a factor further enhanced by the tethering of ovoperoxidase to this matrix by proteoliaisin (Somers et al., 1989). Thus, substrate specificity and the quantity of total residues affected (one-crosslink per 50-100 kDa total protein) (Foerder and Shapiro, 1977; Hall, 1978) are likely to be essential for maintaining fertilization envelope permeability until hatching.

Together, profiling in vivo ovoperoxidase activity and identifying its targets enable the integration of enzymatic activities and structural protein interactions within the temporal dynamics of cell surface changes during the egg-to-embryo transition (Fig. 6). (1) Cortical granule exocytosis releases the serine protease CGSP1 and ovoperoxidase along with the major structural proteins (Wong and Wessel, 2006a). (2) Environmental alkalination auto-activates these cortical granule-derived proenzymes over different time frames (Deits and Shapiro, 1985; Haley and Wessel, 2004b). CGSP1 activates first, and proceeds to (3) cleave the microvillar protein p160 (Haley and Wessel, 1999; Haley and Wessel, 2004a), freeing the vitelline layer so that it separates from the plasma membrane by the hydrating force of cortical granule-derived mucopolysaccharides released between the zygotic hyaline layer and the fertilization envelope (Harvey, 1909; Larabell and Chandler, 1991). (4) Egg surface transglutaminase at the microvillar caps crosslinks local glutamines and lysines (Battaglia and Shapiro, 1988). This activity requires cortical granule exocytosis, suggesting that CGSP1 proteolysis may activate zymogenic transglutaminase – similar to the activity of thrombin on factor XIIIa during blood clotting (Verderio et al., 2004). Transamidation tapers (Battaglia and Shapiro, 1988) as (5) synthesis of hydrogen peroxide by Udx1 peaks (Wong et al., 2004) and ovoperoxidase overcomes its pH-dependent conformational hysteresis (Deits and Shapiro, 1985; Deits and

Shapiro, 1986). These coordinated events provide optimal rates of dityrosine crosslinking, resulting in covalent bonding of 13-15% of all available tyrosyl residues within the fertilization envelope (Foerder and Shapiro, 1977; Hall, 1978). (6) Covalent crosslinking activity mostly affects the ovoperoxidase-tether proteoliaisin and its direct binding partner, the vitelline layer-associated isoform of rendezvin (RDZ[120]), which preferentially associates with the other low-density lipoprotein type A (LDLrA) repeat-containing proteins SFE1 and SFE9 (Mozingo et al., 1994; Somers and Shapiro, 1991; Weidman et al., 1985; Wong and Wessel, 2006b). This local clustering of target proteins within discrete zones within the fertilization envelope (Kay and Shapiro, 1987; Mozingo and Chandler, 1991; Mozingo et al., 1994; Somers and Shapiro, 1989) is likely to be a major contributor to the selectivity of ovoperoxidase, although CGSP1 and transglutaminase may have also modified the matrix sufficiently to restrict access of ovoperoxidase to other proteins, including the cortical granule rendezvin components RDZ[60] and RDZ[90]. After 2 minutes of peak activity, repression of Udx1 (Wong et al., 2004) and prolonged CGSP1 activity (Haley and Wessel, 2004b) together inhibit further crosslinking. Thus, the tight regulation of ovoperoxidase activity and restricted localization together transform the uniform matrix assembly into a barrier that encloses the embryo in a microenvironment critical for development.

Supplementary material
Supplementary material for this article is available at
http://dev.biologists.org/cgi/content/full/135/3/431/DC1

References

Ambati, J., Canakis, C. S., Miller, J. W., Gragoudas, E. S., Edwards, A., Weissgold, D. J., Kim, I., Delori, F. C. and Adamis, A. P. (2000). Diffusion of high molecular weight compounds through sclera. *Invest. Ophthalmol. Vis. Sci.* **41**, 1181-1185.

Barrett, D., Edwards, B. F., Wood, D. B. and Lane, D. J. (1971). Physical heterogeneity of hatching enzyme of the sea urchin, Strongylocentrotus purpuratus. *Arch. Biochem. Biophys.* **143**, 261-268.

Battaglia, D. E. and Shapiro, B. M. (1988). Hierarchies of protein cross-linking in the extracellular matrix: involvement of an egg surface transglutaminase in early stages of fertilization envelope assembly. *J. Cell Biol.* **107**, 2447-2454.

Bauskin, A. R., Franken, D. R., Eberspaecher, U. and Donner, P. (1999). Characterization of human zona pellucida glycoproteins. *Mol. Hum. Reprod.* **5**, 534-540.

Bergendi, L., Benes, L., Durackova, Z. and Ferencik, M. (1999). Chemistry, physiology and pathology of free radicals. *Life Sci.* **65**, 1865-1874.

Bobrow, M. N., Harris, T. D., Shaughnessy, K. J. and Litt, G. J. (1989). Catalyzed reporter deposition, a novel method of signal amplification. Application to immunoassays. *J. Immunol. Methods* **125**, 279-285.

Bobrow, M. N., Shaughnessy, K. J. and Litt, G. J. (1991). Catalyzed reporter deposition, a novel method of signal amplification. II. Application to membrane immunoassays. *J. Immunol. Methods* **137**, 103-112.

Carroll, D. J., Acevedo-Duncan, M., Justice, R. W. and Santiago, L. (1986). Structure, assembly and function of the surface envelope (fertilization envelope) from eggs of the sea urchins, Strongylocentrotus purpuratus. *Adv. Exp. Med. Biol.* **207**, 261-291.

Chang, Y. S., Wang, Y. W. and Huang, F. L. (2002). Cross-linking of ZP2 and ZP3 by transglutaminase is required for the formation of the outer layer of fertilization envelope of carp egg. *Mol. Reprod. Dev.* **63**, 237-244.

Cheng, S. D., Glas, P. S. and Green, J. D. (1991). Abnormal sea urchin fertilization envelope assembly in low sodium seawater. *Biol. Bull.* **180**, 346-354.

D'Aniello, A., de Vincentiis, M., Di Fiore, M. M. and Scippa, S. (1997). Hatching enzyme from the sea-squirt Ciona intestinalis: purification and properties. *Biochim. Biophys. Acta* **1339**, 101-112.

Davies, K. J. (1987). Protein damage and degradation by oxygen radicals. I. General aspects. *J. Biol. Chem.* **262**, 9895-9901.

Davies, K. J. and Delsignore, M. E. (1987). Protein damage and degradation by oxygen radicals. III. Modification of secondary and tertiary structure. *J. Biol. Chem.* **262**, 9908-9913.

Davies, K. J., Delsignore, M. E. and Lin, S. W. (1987). Protein damage and degradation by oxygen radicals. II. Modification of amino acids. *J. Biol. Chem.* **262**, 9902-9907.

Deits, T. and Shapiro, B. M. (1985). pH-induced hysteretic transitions of ovoperoxidase. *J. Biol. Chem.* **260**, 7882-7888.

Deits, T. L. and Shapiro, B. M. (1986). Conformational control of ovoperoxidase catalysis in the sea urchin fertilization membrane. *J. Biol. Chem.* **261**, 12159-12165.

Dunn, T. J. and Dunn, A. D. (2001). Update on intrathyroidal iodine metabolism. *Thyroid* **11**, 407-414.

Edens, W. A., Sharling, L., Cheng, G., Shapira, R., Kinkade, J. M., Lee, T., Edens, H. A., Tang, X., Sullards, C., Flaherty, D. B. et al. (2001). Tyrosine cross-linking of extracellular matrix is catalyzed by Duox, a multidomain oxidase/peroxidase with homology to the phagocyte oxidase subunit gp91phox. *J. Cell Biol.* **154**, 879-891.

Fan, T. J. and Katagiri, C. (2001). Properties of the hatching enzyme from Xenopus laevis. *Eur. J. Biochem.* **268**, 4892-4898.

Foerder, C. A. and Shapiro, B. M. (1977). Release of ovoperoxidase from sea urchin eggs hardens the fertilization membrane with tyrosine crosslinks. *Proc. Natl. Acad. Sci. USA* **74**, 4214-4218.

Fridovich, I. (1998). Oxygen toxicity: a radical explanation. *J. Exp. Biol.* **201**, 1203-1209.

Grey, R. D., Wolf, D. P. and Hedrick, J. L. (1974). Formation and structure of the fertilization envelope in Xenopus laevis. *Dev. Biol.* **36**, 44-61.

Gross, A. J. (1959). The oxidation of tyramine, tyrosine, and related compounds by peroxidase. *J. Biol. Chem.* **234**, 1611-1614.

Gulyas, B. J. and Schmell, E. D. (1980). Ovoperoxidase activity in ionophore-treated mouse eggs. II. Evidence for the enzyme's role in hardening the zona pellucida. *Gamete Res.* **3**, 279-290.

Ha, C. R. and Iuchi, I. (1998). Enzyme responsible for egg envelope (chorion) hardening in fish: purification and partial characterization of two transglutaminases associated with their substrate, unfertilized egg chorion, of the rainbow trout, Oncorhynchus mykiss. *J. Biochem.* **124**, 917-926.

Haley, S. A. and Wessel, G. M. (1999). The cortical granule serine protease CGSP1 of the sea urchin, Strongylocentrotus purpuratus, is autocatalytic and contains a low-density lipoprotein receptor-like domain. *Dev. Biol.* **211**, 1-10.

Haley, S. A. and Wessel, G. M. (2004a). Proteolytic cleavage of the cell surface protein p160 is required for detachment of the fertilization envelope in the sea urchin. *Dev. Biol.* **272**, 191-202.

Haley, S. A. and Wessel, G. M. (2004b). Regulated proteolysis by cortical granule serine protease 1 at fertilization. *Mol. Biol. Cell* **15**, 2084-2092.

Hall, H. G. (1978). Hardening of the sea urchin fertilization envelope by peroxidase-catalyzed phenolic coupling of tyrosines. *Cell* **15**, 343-355.

Harvey, E. N. (1909). The mechanism of membrane formation and other early changes in developing sea urchins' eggs as bearing on the problem of artificial parthenogenesis. *J. Exp. Zool.* **8**, 355-376.

Heinecke, J. W. (1999). Mass spectrometric quantification of amino acid oxidation products in proteins: insights into pathways that promote LDL oxidation in the human artery wall. *FASEB J.* **13**, 1113-1120.

Heinecke, J. W., Li, W., Daehnke, H. L., 3rd and Goldstein, J. A. (1993a). Dityrosine, a specific marker of oxidation, is synthesized by the myeloperoxidase-hydrogen peroxide system of human neutrophils and macrophages. *J. Biol. Chem.* **268**, 4069-4077.

Heinecke, J. W., Li, W., Francis, G. A. and Goldstein, J. A. (1993b). Tyrosyl radical generated by myeloperoxidase catalyzes the oxidative cross-linking of proteins. *J. Clin. Invest.* **91**, 2866-2872.

Hunyady, B., Krempels, K., Harta, G. and Mezey, E. (1996). Immunohistochemical signal amplification by catalyzed reporter deposition and its application in double immunostaining. *J. Histochem. Cytochem.* **44**, 1353-1362.

Jacob, J. S., Cistola, D. P., Hsu, F. F., Muzaffar, S., Mueller, D. M., Hazen, S. L. and Heinecke, J. W. (1996). Human phagocytes employ the myeloperoxidase-hydrogen peroxide system to synthesize dityrosine, trityrosine, pulcherosine, and isodityrosine by a tyrosyl radical-dependent pathway. *J. Biol. Chem.* **271**, 19950-19956.

Josic, D., Brown, M. K., Huang, F., Callanan, H., Rucevic, M., Nicoletti, A., Clifton, J. and Hixson, D. C. (2005). Use of selective extraction and fast chromatographic separation combined with electrophoretic methods for mapping of membrane proteins. *Electrophoresis* **26**, 2809-2822.

Josic, D., Brown, M. K., Huang, F., Lim, Y. P., Rucevic, M., Clifton, J. G. and Hixson, D. C. (2006). Proteomic characterization of inter-alpha inhibitor proteins from human plasma. *Proteomics* **6**, 2874-2885.

Katagiri, C., Maeda, R., Yamashika, C., Mita, K., Sargent, T. D. and Yasumasu, S. (1997). Molecular cloning of Xenopus hatching enzyme and its specific expression in hatching gland cells. *Int. J. Dev. Biol.* **41**, 19-25.

Kay, E. S. and Shapiro, B. M. (1985). The formation of the fertilization membrane of the sea urchin egg. In *Biology of Fertilization*. Vol. 3 (ed. C. B. Metz and A. Monroy), pp. 45-80. Orlando, FL: Academic Press.

Kay, E. S. and Shapiro, B. M. (1987). Ovoperoxidase assembly into the sea urchin fertilization envelope and dityrosine crosslinking. *Dev. Biol.* **121**, 325-334.

Kiehart, D. P. (1982). Microinjection of echinoderm eggs: apparatus and procedures. In *Methods in Cell Biology*. Vol. 25, Pt B (ed. L. Wilson), pp. 13-31. New York, NY: Academic Press.

Kitamura, Y. and Katagiri, C. (1998). Characterization of the hatching enzyme from embryos of an anuran amphibian, Rana pirica. *Biochim. Biophys. Acta* **1387**, 153-164.

Klebanoff, S. J., Foerder, C. A., Eddy, E. M. and Shapiro, B. M. (1979). Metabolic similarities between fertilization and phagocytosis. Conservation of a peroxidatic mechanism. *J. Exp. Med.* **149**, 938-953.

Kudo, S. (1988). Chorionic peroxidase activity in the eggs of the fish Tribolodon hakonesis. *J. Exp. Zool.* **245**, 63-70.

LaFleur, G. J., Jr, Horiuchi, Y. and Wessel, G. M. (1998). Sea urchin ovoperoxidase: oocyte-specific member of a heme-dependent peroxidase superfamily that functions in the block to polyspermy. *Mech. Dev.* **70**, 77-89.

Larabell, C. and Chandler, D. E. (1991). Fertilization-induced changes in the vitelline envelope of echinoderm and amphibian eggs: self-assembly of an extracellular matrix. *J. Electron Microsc. Tech.* **17**, 294-318.

Larios, J. M., Budhiraja, R., Fanburg, B. L. and Thannickal, V. J. (2001). Oxidative protein cross-linking reactions involving L-tyrosine in transforming growth factor-beta1-stimulated fibroblasts. *J. Biol. Chem.* **276**, 17437-17441.

Lee, K. S., Yasumasu, S., Nomura, K. and Iuchi, I. (1994). HCE, a constituent of the hatching enzymes of Oryzias latipes embryos, releases unique proline-rich polypeptides from its natural substrate, the hardened chorion. *FEBS Lett.* **339**, 281-284.

Lepage, T. and Gache, C. (1990). Early expression of a collagenase-like hatching enzyme gene in the sea urchin embryo. *EMBO J.* **9**, 3003-3012.

Levine, R. L. and Stadtman, E. R. (2001). Oxidative modification of proteins during aging. *Exp. Gerontol.* **36**, 1495-1502.

Li, J., Hodgeman, B. A. and Christensen, B. M. (1996). Involvement of peroxidase in chorion hardening in Aedes aegypti. *Insect Biochem. Mol. Biol.* **26**, 309-317.

Lindsay, L. L. and Hedrick, J. L. (2004). Proteolysis of Xenopus laevis egg envelope ZPA triggers envelope hardening. *Biochem. Biophys. Res. Commun.* **324**, 648-654.

Linton, S., Davies, M. J. and Dean, R. T. (2001). Protein oxidation and ageing. *Exp. Gerontol.* **36**, 1503-1518.

Lorand, L. and Graham, R. M. (2003). Transglutaminases: crosslinking enzymes with pleiotropic functions. *Nat. Rev. Mol. Cell Biol.* **4**, 140-156.

McGadey, J. (1970). A tetrazolium method for non-specific alkaline phosphatase. *Histochemie* **23**, 180-184.

Moller, C. C. and Wassarman, P. M. (1989). Characterization of a proteinase that

cleaves zona pellucida glycoprotein ZP2 following activation of mouse eggs. *Dev. Biol.* **132**, 103-112.

Morrison, M. and Schonbaum, G. R. (1976). Peroxidase-catalyzed halogenation. *Annu. Rev. Biochem.* **45**, 861-888.

Mozingo, N. M. and Chandler, D. E. (1991). Evidence for the existence of two assembly domains within the sea urchin fertilization envelope. *Dev. Biol.* **146**, 148-157.

Mozingo, N. M., Hollar, L. R. and Chandler, D. E. (1993). Degradation of an extracellular matrix: sea urchin hatching enzyme removes cortical granule-derived proteins from the fertilization envelope. *J. Cell Sci.* **104**, 929-938.

Mozingo, N. M., Somers, C. E. and Chandler, D. E. (1994). Ultrastructure of the proteoliaisin-ovoperoxidase complex and its spatial organization within the Strongylocentrotus purpuratus fertilization envelope. *J. Cell Sci.* **107**, 2769-2777.

Nomura, K., Shimizu, T., Kinoh, H., Sendai, Y., Inomata, M. and Suzuki, N. (1997). Sea urchin hatching enzyme (envelysin): cDNA cloning and deprivation of protein substrate specificity by autolytic degradation. *Biochemistry* **36**, 7225-7238.

Oppen-Berntsen, D. O., Helvik, J. V. and Walther, B. T. (1990). The major structural proteins of cod (Gadus morhua) eggshells and protein crosslinking during teleost egg hardening. *Dev. Biol.* **137**, 258-265.

Parr, M. B. and Parr, E. L. (1986). Permeability of the primary decidual zone in the rat uterus: studies using fluorescein-labeled proteins and dextrans. *Biol. Reprod.* **34**, 393-403.

Perkins, D. N., Pappin, D. J., Creasy, D. M. and Cottrell, J. S. (1999). Probability-based protein identification by searching sequence databases using mass spectrometry data. *Electrophoresis* **20**, 3551-3567.

Persky, B. and Hendrix, M. J. (1990). Artificial matrix barriers: a diffusion study utilizing dextrans and microspheres. *Anat. Rec.* **228**, 15-22.

Sawada, H., Yamazaki, K. and Hoshi, M. (1990). Trypsin-like hatching protease from mouse embryos: evidence for the presence in culture medium and its enzymatic properties. *J. Exp. Zool.* **254**, 83-87.

Schuel, H., Kelly, J. W., Berger, E. R. and Wilson, W. L. (1974). Sulfated acid mucopolysaccharides in the cortical granules of eggs. Effects of quaternary ammonium salts on fertilization. *Exp. Cell Res.* **88**, 24-30.

Shapiro, B. M., Somers, C. E. and Weidman, P. J. (1989). Extracellular remodeling during fertilization. In *The Cell Biology of Fertilization* (ed. H. Schatten and G. Schatten), pp. 251-276. San Diego: Academic Press.

Showman, R. M. and Foerder, C. A. (1979). Removal of the fertilization membrane of sea urchin embryos employing aminotriazole. *Exp. Cell Res.* **120**, 253-255.

Somers, C. E. and Shapiro, B. M. (1989). The heme environment of ovoperoxidase as determined by optical spectroscopy. *J. Biol. Chem.* **264**, 17231-17235.

Somers, C. E. and Shapiro, B. M. (1991). Functional domains of proteoliaisin, the adhesive protein that orchestrates fertilization envelope assembly. *J. Biol. Chem.* **266**, 16870-16875.

Somers, C. E., Battaglia, D. E. and Shapiro, B. M. (1989). Localization and

developmental fate of ovoperoxidase and proteoliaisin, two proteins involved in fertilization envelope assembly. *Dev. Biol.* **131**, 226-235.

Talbot, P. and Goudeau, M. (1988). A complex cortical reaction leads to formation of the fertilization envelope in the lobster, Homarus. *Gamete Res.* **19**, 1-18.

Talbot, P. and Dandekar, P. (2003). Perivitelline space: does it play a role in blocking polyspermy in mammals? *Microsc. Res. Tech.* **61**, 349-357.

Verderio, E. A., Johnson, T. and Griffin, M. (2004). Tissue transglutaminase in normal and abnormal wound healing: review article. *Amino Acids* **26**, 387-404.

Voronina, E. and Wessel, G. M. (2004). betagamma subunits of heterotrimeric G-proteins contribute to Ca^{2+} release at fertilization in the sea urchin. *J. Cell Sci.* **117**, 5995-6005.

Weidman, P. J., Kay, E. S. and Shapiro, B. M. (1985). Assembly of the sea urchin fertilization membrane: isolation of proteoliaisin, a calcium-dependent ovoperoxidase binding protein. *J. Cell Biol.* **100**, 938-946.

Wessel, G. M. (1995). A protein of the sea urchin cortical granules is targeted to the fertilization envelope and contains an LDL-receptor-like motif. *Dev. Biol.* **167**, 388-397.

Wessel, G. M., Conner, S., Laidlaw, M., Harrison, J. and LaFleur, G. J., Jr (2000a). SFE1, a constituent of the fertilization envelope in the sea urchin is made by oocytes and contains low-density lipoprotein-receptor-like repeats. *Biol. Reprod.* **63**, 1706-1712.

Wessel, G. M., Zaydfudim, V., Hsu, Y. J., Laidlaw, M. and Brooks, J. M. (2000b). Direct molecular interaction of a conserved yolk granule protein in sea urchins. *Dev. Growth Differ.* **42**, 507-517.

Wilm, M., Shevchenko, A., Houthaeve, T., Breit, S., Schweigerer, L., Fotsis, T. and Mann, M. (1996). Femtomole sequencing of proteins from polyacrylamide gels by nano-electrospray mass spectrometry. *Nature* **379**, 466-469.

Wong, J. L. and Wessel, G. M. (2004). Major components of a sea urchin block to polyspermy are structurally and functionally conserved. *Evol. Dev.* **6**, 134-153.

Wong, J. L. and Wessel, G. M. (2005). Reactive oxygen species and Udx1 during early sea urchin development. *Dev. Biol.* **288**, 317-333.

Wong, J. L. and Wessel, G. M. (2006a). Defending the zygote: search for the ancestral animal block to polyspermy. *Curr. Top. Dev. Biol.* **72**, 1-151.

Wong, J. L. and Wessel, G. M. (2006b). Rendezvin: an essential gene encoding independent, differentially-secreted egg proteins that organize the fertilization envelope proteome following self-association. *Mol. Biol. Cell* **17**, 5241-5252.

Wong, J. L., Créton, R. and Wessel, G. M. (2004). The oxidative burst at fertilization is dependent upon activation of the dual oxidase Udx1. *Dev. Cell* **7**, 801-814.

Yamagami, K., Hamazaki, T. S., Yasumasu, S., Masuda, K. and Iuchi, I. (1992). Molecular and cellular basis of formation, hardening, and breakdown of the egg envelope in fish. *Int. Rev. Cytol.* **136**, 51-92.

Yip, C. C. (1966). The iodination of tyrosine by myeloperoxidase and beef thyroids: the possible involvement of free radicals. *Biochim. Biophys. Acta* **122**, 406-412.

Zanetti, L., Ristoratore, F., Bertoni, A. and Cariello, L. (2004). Characterization of sea urchin transglutaminase, a protein regulated by guanine/adenine nucleotides. *J. Biol. Chem.* **279**, 49289-49297.